

Spectroelectrochemical (Electronic and FTIR) Studies of Tris(maleonitriledithiolate) Complexes

Stephen P. Best,* Robin J. H. Clark,* Roderick C. S. McQueen, and Jacqueline R. Walton

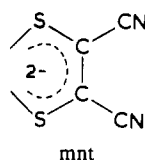
Received July 10, 1987

Spectroelectrochemical studies of tris(maleonitriledithiolate) complexes, $[M(\text{mnt})_3]^{z-}$, of vanadium, chromium, manganese, iron, molybdenum, tungsten, and rhenium have led to the electronic and FTIR characterization of species with z ranging from 1 to 3. In particular, the FTIR studies have defined in detail the manner in which $\nu(\text{CN})$ varies with charge. For the range of complexes studied, $\nu(\text{CN}) = 2215.7 \pm 2 \text{ cm}^{-1}$ for $z = 1$, $2202.1 \pm 2 \text{ cm}^{-1}$ for $z = 2$, and $2183 \pm 13 \text{ cm}^{-1}$ for $z = 3$. For the complexes with $z = 1$ or 2, the insensitivity of $\nu(\text{CN})$ to the identity of the metal indicates that there are no significant π interactions between the metal and ligand orbitals and that the stability of the complex ions is largely a consequence of strong metal-sulfur σ bonding. For $z = 3$, however, significant metal-ligand π back-bonding occurs. The relationship between molecular geometry, charge, and electronic structure is discussed.

Introduction

Sulfur chelate donors readily form complexes with a range of transition metals that are generally characterized by a rich redox chemistry.¹⁻⁶ In such complexes overlap between ligand and metal orbitals facilitates the redistribution of charge throughout the complex to the extent that the formal oxidation state of the metal ion is a notional term. Our interest lies in understanding the factors that (a) determine the redistribution of charge on a complex with oxidation or reduction and that (b) lead to any consequent changes in structure.

Intensive studies of *cis*-1,2-dicyano-1,2-ethylenedithiolate, maleonitriledithiolate (mnt), were first initiated by Gray and co-workers in 1962.¹ The tris-ligand complexes are typical of



dithiolates, being intensely colored, stable redox-active materials.

This work is concerned with some spectroelectrochemical studies of $(\text{mnt})_3$ complexes of several transition-metal ions in the UV/visible and IR regions, the latter using a newly designed infrared reflection-absorption spectroscopy (IRRAS) cell.⁷ Correlations between the IR absorption band maxima (principally $\nu(\text{CN})$) and the structure, charge, and electronic configuration are discussed.

Experimental Section

The complexes $[\text{AsPh}_4]_2[\text{V}(\text{mnt})_3]$,⁸ $[\text{PPh}_4]_3[\text{Cr}(\text{mnt})_3]$,⁸ $[\text{PPh}_4]_2[\text{Mn}(\text{mnt})_3]$,¹ $[\text{PPh}_4]_2[\text{Fe}(\text{mnt})_3]$,¹ $[\text{NBu}_4]_2[\text{Mo}(\text{mnt})_3]$,⁸ $[\text{PPh}_4]_2[\text{W}(\text{mnt})_3]$,⁸ and $[\text{PPh}_4]_2[\text{Re}(\text{mnt})_3]$ ⁹ were all prepared by literature methods and were shown to be pure by elemental analysis (C, H, N, and S).

Tetra-*n*-butylammonium tetrafluoroborate, $[\text{Bu}_4\text{N}][\text{BF}_4]$, was prepared by the neutralization of the appropriate hydroxide with tetrafluoroboric acid, recrystallized from MeOH/H₂O, and dried under vacuum (80 °C, 0.1 Torr) for 24 h before use. Dichloromethane was dried by distillation from P₂O₅ and stored under nitrogen prior to use.

Electrochemical experiments were carried out by using a Metrohm E506 potentiostat and Metrohm E612 VA scanner. Platinum wires were

Table I. Redox Potentials of Complexes $[M(\text{mnt})_3]^{z-}$ ^a

M	couple		
	0/1-	1-/2-	2-/3-
V ^c		+0.70	-0.35
Cr		+0.66 ^b	+0.17
Mn			-0.05
Fe ^c			-0.07
Mo ^c	+1.28	+0.73	-0.95
W		+0.68 ^b	-1.16
Re		+0.17	-0.59

^a 0.2 M $[(n\text{-C}_4\text{H}_9)_4\text{N}]\text{BF}_4/\text{CH}_2\text{Cl}_2$ and 20 °C; E° in volts with respect to Ag/AgCl. ^b Irreversible at 20 °C; reversible at -20 °C. ^c Further irreversible redox step observed; see text.

used as working and counter electrodes for voltammetric experiments, while the reference electrode was an Ag/AgCl system (Metrohm EA441/5); all redox potentials are quoted with respect to this electrode. All results were cross-referenced by using the ferrocene/ferrocenium couple as a calibrant. The oxidation of $\text{Fe}(\text{cp})_2$ occurs at +0.50 V with respect to Ag/AgCl.

Electronic spectra were recorded by using a Varian 2390 spectrometer. An optically transparent thin-layer electrode (OTTLE) cell based on the design of Heath¹⁰ was used for all electronic spectroelectrochemical experiments. A platinum minigrad OTTLE mounted in a gastight polytetrafluoroethylene cell block held in the spectrometer beam was used for all electrolyses. For low-temperature work a stream of nitrogen, cooled by passage through a heat exchanger maintained at liquid-nitrogen temperature, was blown over the faces of the cell. The spectrometer compartment was flushed continuously with dry nitrogen while a stream of nitrogen directed over the cell block prevented condensation forming on the cell windows. By adjustment of the relative gas flow rates the temperature in the cell could be kept constant within ± 1 K.

IR spectra were recorded by using a Bruker 113V Fourier transform interferometer equipped with a liquid-nitrogen-cooled detector and a Ge-coated KBr beam splitter. The IRRAS cell used in this study has been described elsewhere.⁷ The IR beam passes through the cell window (KBr for mid-IR studies, CsI for far-IR) and into a thin layer of solution and is then reflected from a highly polished disk of platinum metal that acts both as working electrode and as reflector. Solution thickness was controlled by using the micrometer. Cooling of the thin film was achieved by passing cold nitrogen gas through the channels in the central brass rod to which the platinum disk is welded.

The detector for far-IR studies was an Infrared Laboratories Model HD-3 liquid-helium-cooled bolometer.

All solutions were degassed with dry oxygen-free nitrogen before use and maintained under a nitrogen atmosphere throughout. Sample concentrations were $\sim 10^{-3} \text{ mol dm}^{-3}$ for UV/visible spectroscopy and $\sim 5 \times 10^{-2} \text{ mol dm}^{-3}$ for infrared spectroelectrochemistry.

Results

The redox behavior of a series of $[M(\text{mnt})_3]^{z-}$ complexes ($M = \text{V}, \text{Cr}, \text{Mn}, \text{Fe}, \text{Mo}, \text{W}, \text{Re}$) in dichloromethane solution has

- Gray, H. B.; Williams, R.; Bernal, I.; Billig, E. J. *Am. Chem. Soc.* **1962**, *84*, 3596.
- Eisenberg, R.; Ibers, J. A.; Clark, R. J. H.; Gray, H. B. *J. Am. Chem. Soc.* **1964**, *86*, 113.
- Shupack, S. I.; Billig, E.; Clark, R. J. H.; Williams, R.; Gray, H. B. *J. Am. Chem. Soc.* **1964**, *86*, 4594.
- Gray, H. B. *Transition Met. Chem. (NY)* **1965**, *1*, 240.
- McCleverty, J. A. *Prog. Inorg. Chem.* **1968**, *10*, 49.
- Burns, R. P.; McAuliffe, C. A. *Adv. Inorg. Chem. Radiochem.* **1979**, *22*, 303.
- Best, S. P.; Clark, R. J. H.; Cooney, R. P.; McQueen, R. C. S. *Rev. Sci. Instrum.* **1987**, *58*, 2071.
- Davison, A.; Edelstein, N.; Holm, R. H.; Maki, A. H. *J. Am. Chem. Soc.* **1964**, *86*, 2799.
- Connelly, N. G.; Jones, G. J.; McCleverty, J. A. *J. Chem. Soc. A* **1971**, 712.

- Heath, G. A.; Lindsay, A. J.; Stephenson, T. A.; Vattis, D. K. *J. Organomet. Chem.* **1982**, *233*, 353.
- Eisenberg, R.; Ibers, J. A. *Inorg. Chem.* **1966**, *5*, 411.
- Cowie, M.; Bennett, M. J. *Inorg. Chem.* **1976**, *15*, 1584, 1589, 1595.

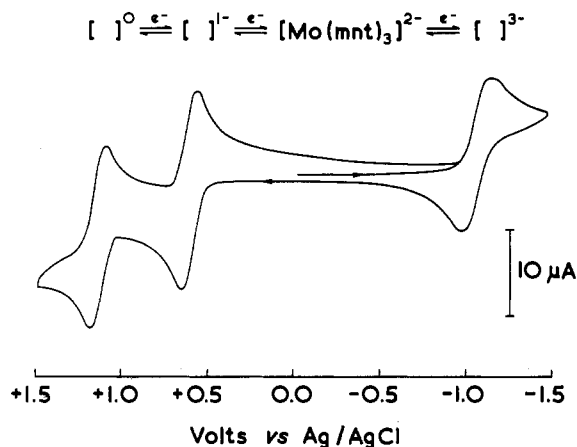


Figure 1. Cyclic voltammogram of $[n\text{-Bu}_4\text{N}]_2[\text{Mo}(\text{mnt})_3]$ (1×10^{-3} mol dm^{-3}) in 0.2 mol dm^{-3} $[n\text{-Bu}_4\text{N}]\text{BF}_4/\text{CH}_2\text{Cl}_2$ (scanning rate 200 mV s^{-1} , Pt working electrode, Ag/AgCl reference electrode).

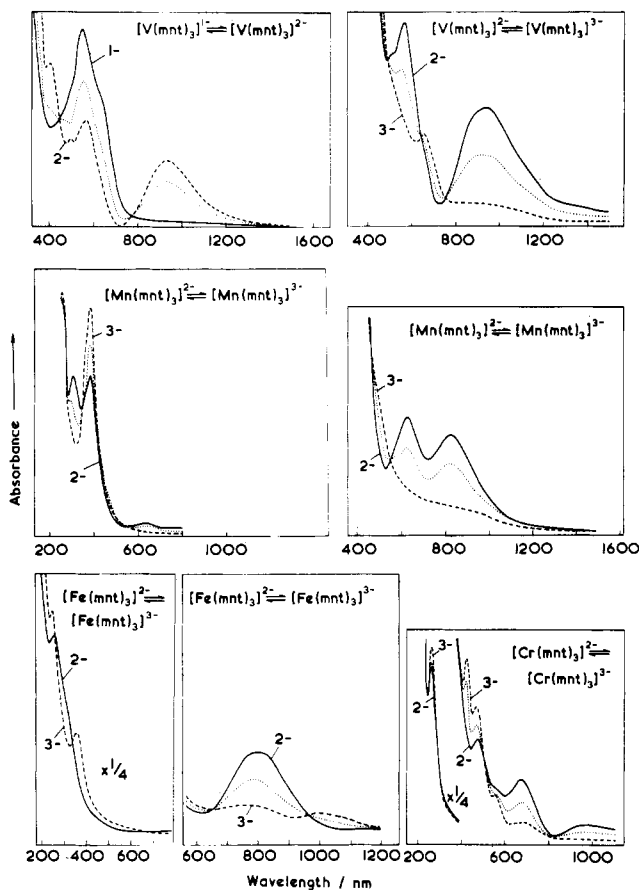


Figure 2. Changes observed in the electronic spectra of $[\text{V}(\text{mnt})_3]^{2-}$, $[\text{Cr}(\text{mnt})_3]^{3-}$, $[\text{Mn}(\text{mnt})_3]^{2-}$, and $[\text{Fe}(\text{mnt})_3]^{2-}$ on oxidation and/or reduction.

been studied. In general, each complex is seen to undergo two or more redox steps in the available potential range, as exemplified by $[\text{Mo}(\text{mnt})_3]^{2-}$ (Figure 1). Redox potentials are given in Table I. In accord with published results,⁵ all the electron-transfer steps studied were verified to be reversible, diffusion-controlled, one-electron processes (e.g. see cyclic voltammogram, Figure 1) under the conditions (room temperature or, in two cases, -20 °C) of the experiment.

In addition to the redox steps noted in Table I, certain complexes were observed to undergo further irreversible electron transfers. Thus the vanadium and molybdenum complexes were observed to be reduced at -1.65 and -1.78 V, respectively, to give a nominal tetraanion. These reductions are apparently reversible under the conditions appropriate for cyclic voltammetry, but preliminary

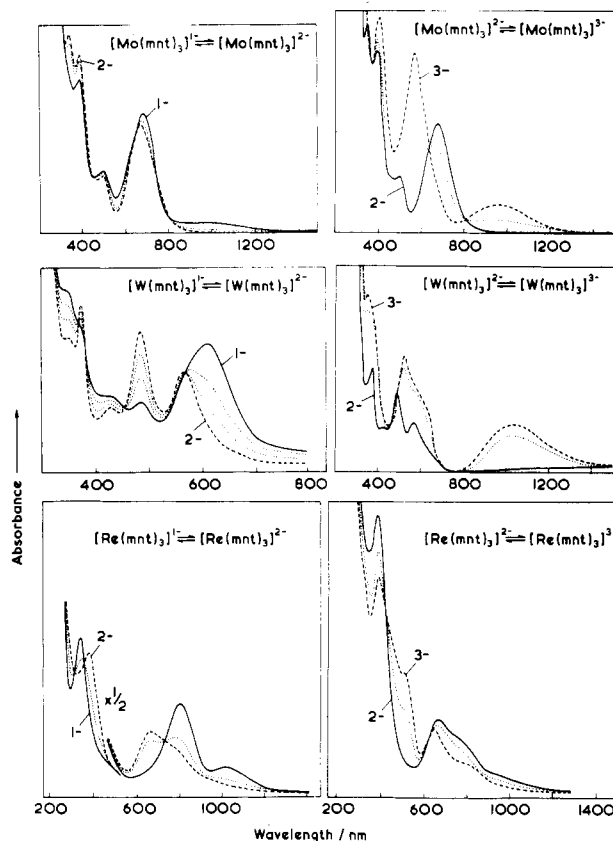


Figure 3. Changes observed in the electronic spectra of $[\text{Mo}(\text{mnt})_3]^{2-}$, $[\text{W}(\text{mnt})_3]^{2-}$, and $[\text{Re}(\text{mnt})_3]^{2-}$ on oxidation and on reduction.

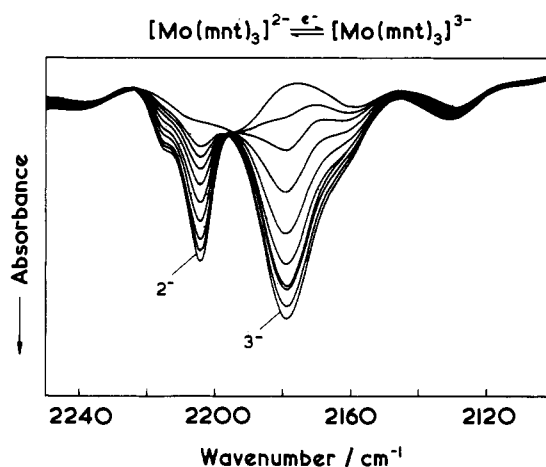


Figure 4. Progression of infrared spectral changes associated with the reduction process $[\text{Mo}(\text{mnt})_3]^{2-} + e^- = [\text{Mo}(\text{mnt})_3]^{3-}$.

studies indicate that rapid polymerization follows reduction to the $[\text{M}(\text{mnt})_3]^{4-}$ species for solutions sufficiently concentrated to permit spectroscopic study ($>10^{-3}$ mol dm^{-3}). In addition to the reversible reduction noted in Table I, the iron complex undergoes further irreversible processes at -0.73 V (reduction) and $+0.78$ V (oxidation). The identity of each of these reaction products is unknown and is still under investigation. Characterization of the species present in solution has been achieved partly by following the development of isosbestic points in the electronic spectra (Figures 2 and 3) and partly by corresponding studies in the infrared spectra—in particular by monitoring changes in $\nu(\text{CN})$. Figure 4 shows the full sequence of spectral changes observed in a typical infrared spectroelectrochemical experiment ($[\text{Mo}(\text{mnt})_3]^{2-} + e^- = [\text{Mo}(\text{mnt})_3]^{3-}$), while in Figures 5–7 we show the initial, one intermediate, and the final spectra observed for each redox process recorded in Table I. Removal of the applied potential results in quantitative regeneration of the starting ma-

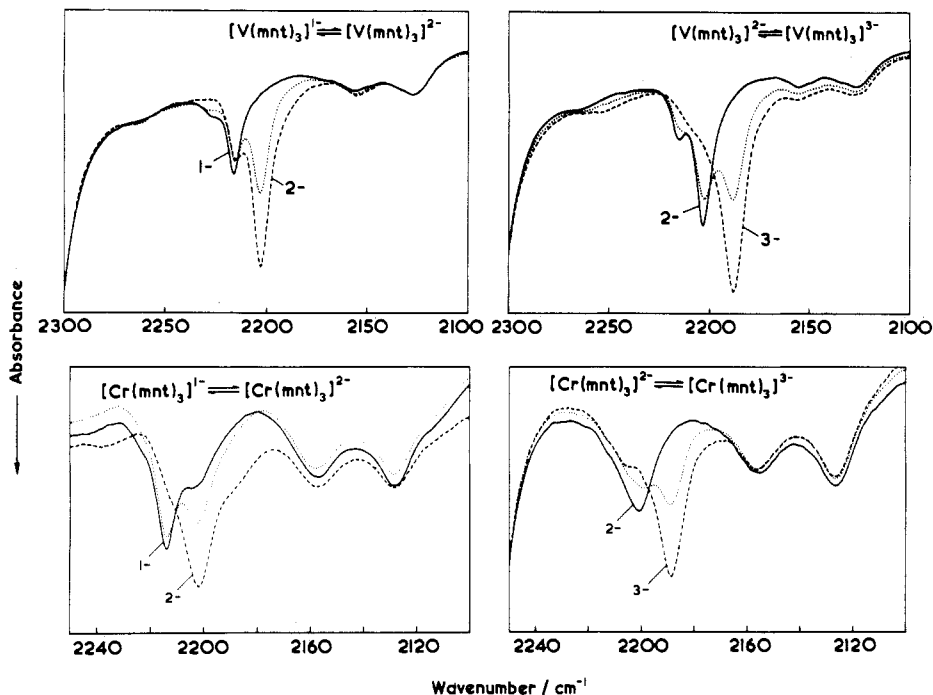


Figure 5. Changes observed in the cyanide stretching frequency of $[\text{V}(\text{mnt})_3]^{2-}$ and $[\text{Cr}(\text{mnt})_3]^{2-}$ on oxidation and on reduction.

Table II. Electronic Maxima/ $10^3 \times \text{cm}^{-1}$ ($\epsilon/\text{dm}^3 \text{mol}^{-1} \text{cm}^{-1}$) of Complexes $[\text{M}(\text{mnt})_3]^{z-}$ ^{a,b}

M	z-		
	1-	2-	3-
V	16.0 (sh, 6200), 18.2 (8900), 20.8 (sh, 5800)	10.7 (2900), 17.6 (4700), 19.9 (3500), 24.4 (6600), 35.0 (21 700)	15.3 (2200), 24.7 (7600)
Cr		10.1 (350), 15.0 (2700), 17.9 (sh, 2300), 20.8 (4500), 36.9 (58 000), 37.7 (63 000)	14.8 (500), 17.9 (1800), 21.4 (6000), 23.8 (8300), 36.8 (65 000), 37.9 (70 000)
Mn		12.0 (2400), 15.7 (2600), 25.8 (36 000), 32.5 (37 000)	25.8 (51 000)
Fe		12.4 (3300), 16.4 (1100), 24.7 (8000), 40.4 (75 000)	10.1 (700), 14.0 (1100), 16.6 (sh, 1200), 27.5 (~37 000), 40.0 (~84 000)
Mo	10.0 (900), 14.5 (7000), 20.3 (3700), 26.0 (8000)	15.0 (5800), 20.2 (2700), 21.7 (2600), 26.0 (10 000), 29.4 (11 000)	10.5 (1450), 18.0 (9500), 25.4 (11 200)
W	16.4 (5700), 20.7 (2800), 23.4 (3200), 27.1 (sh) ^c	17.7 (4000), 20.6 (6700), 24.0 (3500), 27.0 (7700), 28.6 (6600), 32.7 (sh, 2500), 39.4 (26 000)	9.6 (2500), 16.1 (sh, 5300), 19.2 (9700), 28.6 (15 100), 37.9 (31 300)
Re	9.7 (1400), 12.4 (4800), 29.0 (17 300)	10.6 (sh, 1100), 14.8 (3750), 26.0 (14 200), 28.6 (sh, 12 300)	11.8 (sh, 1300), 15.6 (3400), 19.5 (6300), 26.3 (11 400)

^aIn $\text{CH}_2\text{Cl}_2/0.2 \text{ M } [(\text{n-C}_4\text{H}_9)_4\text{N}]\text{BF}_4$. ^bsh = shoulder. ^cRecorded at -20°C .

Table III. Infrared Band Maxima ($\bar{\nu}/\text{cm}^{-1}$) for Complexes $[\text{M}(\text{mnt})_3]^{z-}$ ^{a,b}

M	band	z-		
		1-	2-	3-
V	$\nu(\text{CN})$	2216.1, 2224 (sh)	2203.1, 2215 (sh)	2188.1
	$\nu(\text{VS})$	374.7, 346.7	354.4, 334	
Cr ^c	$\nu(\text{CN})$	2213.7	2202.6	2190.5
Mn	$\nu(\text{CN})$		2201.2, 2211 (sh)	2192.3, 2205.2 (sh)
	$\nu(\text{MnS})$		348.9	328.1
Fe	$\nu(\text{CN})$		2200.0, 2211 (sh)	2185.3
Mo	$\nu(\text{CN})$	2215.6, 2224 (sh)	2202.6, 2213 (sh)	2177.5
W	$\nu(\text{CN})$	2216.9, 2225 (sh)	2202.4, 2213 (sh)	2169.8, 2193 (sh)
Re	$\nu(\text{CN})$	2216.1, 2226 (sh)	2202.7, 2218 (sh)	2178.8, 2200 (sh)
	$\nu(\text{ReS})$	340.2	321.4, 308.1 (sh)	294.1

^aRecorded in $\text{CH}_2\text{Cl}_2/0.2 \text{ M } [(\text{n-C}_4\text{H}_9)_4\text{N}]\text{BF}_4$. ^bsh = shoulder. ^cIn CH_2Cl_2 at -20°C .

terial in all cases. Investigations of changes in the M-S stretching frequency, $\nu(\text{MS})$, have also been undertaken, and the results in a few cases are illustrated in Figure 8; $\nu(\text{MS})$ is clearly sensitive to the formal oxidation state of the metal ion, as expected on the basis of many previous studies of metal-ligand stretching frequencies.

Peak maxima for infrared and electronic spectra are given in Tables II and III, respectively. The experimental conditions

relevant to the spectra in Figures 5-7 are as specified in Table III (footnote).

Discussion

Geometric and Electronic Structures. The coordination geometry of $(\text{mnt})_3$ complexes $[\text{M}(\text{mnt})_3]^{z-}$ may be expected to vary between trigonal prismatic and octahedral, depending on the magnitude of the negative charge carried by the anion and possibly

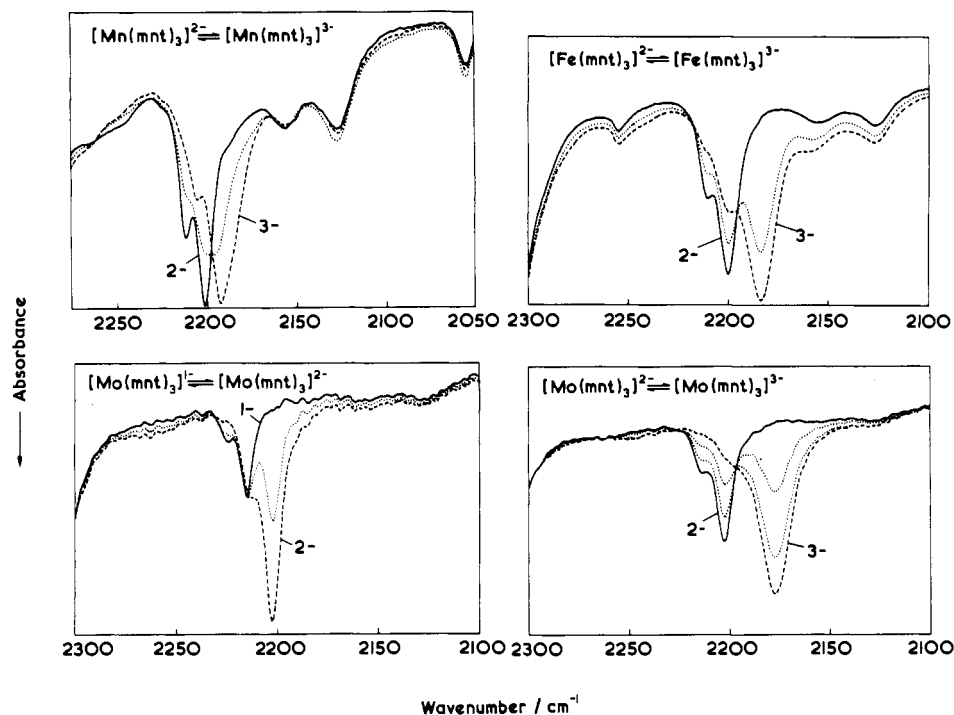


Figure 6. Changes observed in the cyanide stretching frequency of $[\text{Mn}(\text{mnt})_3]^{2-}$, $[\text{Fe}(\text{mnt})_3]^{2-}$, and $[\text{Mo}(\text{mnt})_3]^{2-}$ on oxidation and/or reduction.

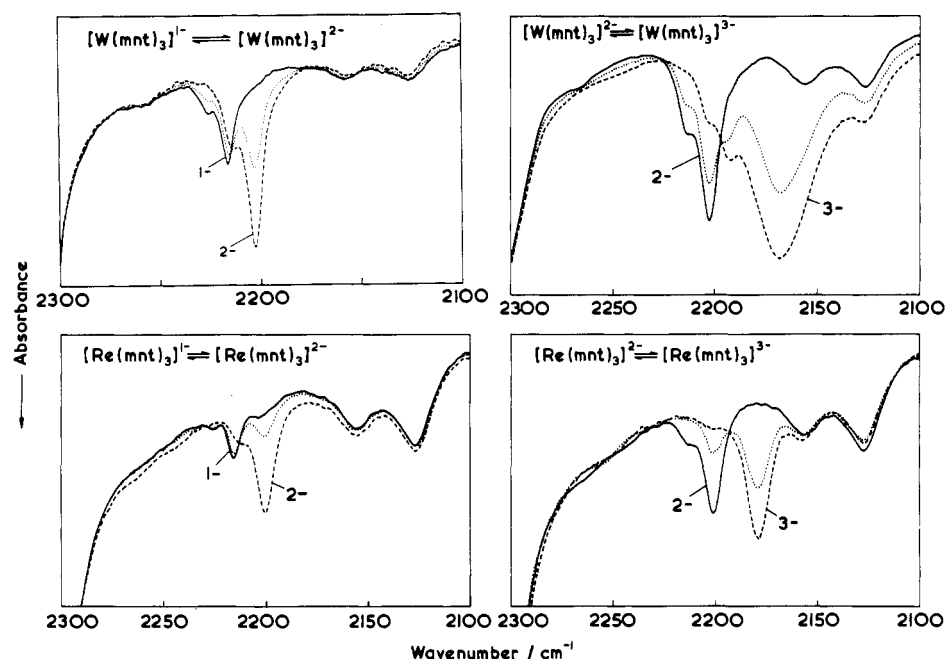


Figure 7. Changes observed in the cyanide stretching frequency of $[\text{W}(\text{mnt})_3]^{2-}$ and $[\text{Re}(\text{mnt})_3]^{2-}$ on oxidation and on reduction.

also on the d-electron occupancy. In practice, the neutral species $[\text{V}(\text{S}_2\text{C}_2\text{Ph}_2)_3]$ (for which there is no known mnt counterpart) has a trigonal-prismatic geometry¹³ that is only slightly distorted toward octahedral by an 8.5° trigonal twist. The dianion $[\text{V}(\text{mnt})_3]^{2-}$ has a structure with D_3 symmetry intermediate between that of the trigonal prism and the octahedron¹⁴ and one that is slightly more distorted in this respect than those of the dianionic molybdenum and tungsten counterparts.¹⁵ It is therefore a moot point as to which geometry should be adopted as a basis for a qualitative description of the electronic structure of the ions. In practice we have chosen that of Stiefel et al.¹⁶ for the trigonal-

prismatic species $\text{Re}(\text{S}_2\text{C}_2\text{Ph}_2)_3$, since it has met with some success in explaining earlier ESR¹⁷ and Raman¹⁸ spectroscopic results.

The key orbitals in this description are $2a_1'$ and $4e'$, which are bonding and which stabilize the trigonal prism, $2a_2'$ which is essentially ligand based ($3\pi_v$) and is nonbonding, and $3a_1'$ and $5e'$, which are antibonding with respect to the trigonal prism (Figure 9a). The $3a_1'$ orbital for such a neutral species is mainly metal based (d_{z^2}) in character, while the $5e'$ orbitals are highly delocalized and of both metal ($d_{x^2-y^2}$, d_{xy}) and ligand ($3\pi_v$) character. On the basis of the scheme outlined above, the redox steps discussed here primarily affect the electronic occupancy of these orbitals. The use of this model is, however, limited to the D_{3h} geometry, and deviations therefrom must affect the relative

(13) Eisenberg, R.; Gray, H. B. *Inorg. Chem.* **1967**, *6*, 1844.

(14) Stiefel, E. I.; Dori, Z.; Gray, H. B. *J. Am. Chem. Soc.* **1967**, *89*, 3353.

(15) Brown, G. F.; Stiefel, E. I. *Inorg. Chem.* **1973**, *12*, 2140.

(16) Stiefel, E. I.; Eisenberg, R.; Rosenberg, R. C.; Gray, H. B. *J. Am. Chem. Soc.* **1966**, *88*, 2956.

(17) Kwik, W. L.; Stiefel, E. I. *Inorg. Chem.* **1973**, *12*, 2337.

(18) Clark, R. J. H.; Turtle, P. C. *J. Chem. Soc., Dalton Trans.* **1978**, 1714.

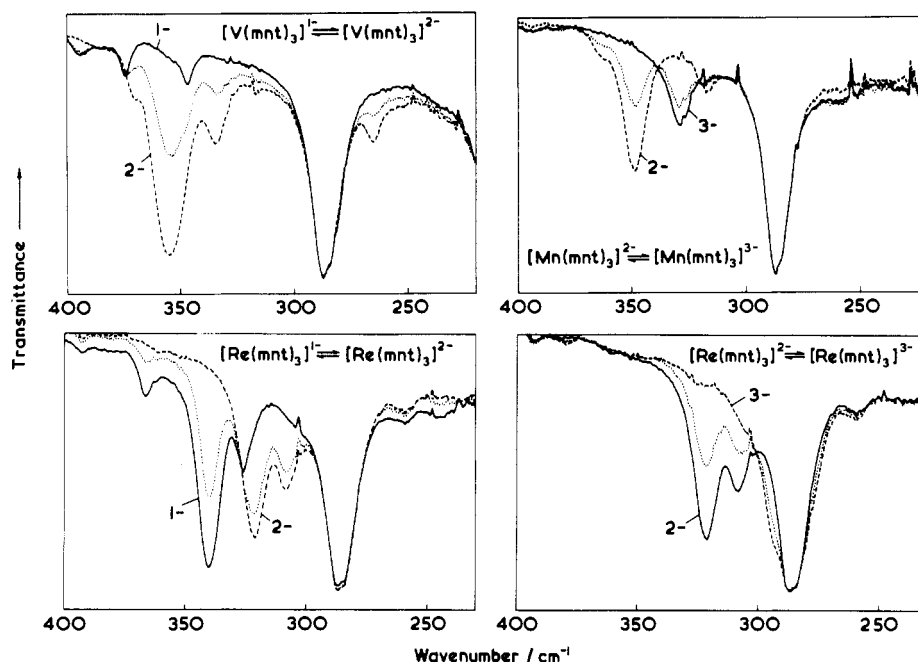


Figure 8. Changes observed in the metal-sulfur stretching frequency of $[\text{V}(\text{mnt})_3]^{2-}$, $[\text{Mn}(\text{mnt})_3]^{2-}$, and $[\text{Re}(\text{mnt})_3]^{2-}$ on oxidation and/or reduction. Liquid-helium-cooled bolometer detection was employed.

energies and symmetries of the molecular orbitals (via a Walsh diagram connecting trigonal-prismatic to octahedral geometries). A limited discussion of molecular orbital energies as a function of geometry in ML_3 complexes has been given by Hoffmann and co-workers for mnt -type complexes¹⁹ as well as for transition-metal dichalcogenides.²⁰ The model adopted involves only a restricted orbital basis set, i.e. one that omits the cyanide orbitals. Although this procedure is clearly incorrect, more detailed MO treatment was not deemed to be worthwhile at this stage, especially since the role played by the cyanide groups is merely to increase the number of π_v orbitals from 4 to 8, where the HOMO, $3\pi_v$, now becomes $5\pi_v$ and the LUMO, $4\pi_v$, becomes $6\pi_v$.²¹

It is particularly important to note that, as $(\text{mnt})_3$ complexes are reduced, the metal orbital energies will be raised (Figure 9b), leading to a significantly different character for the metal-based molecular orbitals in the complexes. This has the consequence that, for the reduced species, π back-bonding from the metal d_x to the ligand π -acceptor orbitals such as $4\pi_v$ (a π orbital that would be antibonding with respect to CN) becomes possible. This has consequences (vide infra) with respect to the $\nu(\text{CN})$ band wavenumbers.

The UV/visible spectra of $(\text{mnt})_3$ complexes are highly sensitive to the identity of the metal atom and to its formal oxidation state (Figures 2 and 3). There is no apparent relationship between the spectra of a series of complexes carrying the same charge, nor even between the spectra of formally isoelectronic complexes. Consequently, we are unable to draw any definite conclusions concerning the electronic structure of the complexes from the UV/visible spectra. The complexity of the spectra and the changes that occur on oxidation or reduction reflect the multiplicity of electronic states, these being highly sensitive to the stereochemistry and to the distribution of charge throughout the complex. From the presence of isosbestic points and from the reversibility of the

spectral changes, we conclude that the electrochemical processes are 1:1 and reversible under the conditions of these experiments (bulk electrolysis, 10^{-3} mol dm^{-3}).

It should be possible to obtain an indication of the geometries of $(\text{mnt})_3$ complexes in solution by monitoring the activities of the cyanide stretching fundamentals in the infrared and Raman spectra. For D_{3h} symmetry, $\Gamma_{\text{CN}} = a_1' + a_2'' + e' + e''$, of which the a_2'' and e' modes are infrared-active and the a_1' , e' , and e'' modes are Raman-active (the e' mode would clearly give rise to a coincidence). For O_h symmetry, $\Gamma_{\text{CN}} = a_{1g} + e_g + t_{1u}$, of which the t_{1u} mode is infrared-active and the a_{1g} and e_g modes are Raman-active (no coincidences). Symmetries lower than D_3 lead not only to an increase in the number of modes active in each case but also to an increase in the number of polarized Raman bands. Unfortunately, it proves to be the case that the Raman spectra of the complexes under study are weak and not strongly enhanced at resonance with accessible electronic bands. Furthermore, the spectra exhibit a strong fluorescence background that swamps the off-resonance Raman spectrum. Hence, it is difficult to detect for certain the number of Raman-active bands in order to carry out this structural exercise. The interpretation to be placed on the presence of a second weak band in the cyanide stretching region is unclear. The magnitude of the splitting between the two $\nu(\text{CN})$ bands follows no set pattern (Table II) and shows no precise correlation with d-electron configuration or residual charge. It is also difficult, therefore, to draw any definite conclusions about molecular geometry from this spectroscopic feature. We are thus obliged to recognize that the precise structures of the $(\text{mnt})_3$ complexes in solution are not known. Fortunately the key conclusions derived from the spectroelectrochemical results do not depend upon this knowledge.

Infrared Spectroelectrochemistry. In principle a full vibrational study should permit the quantification of the force constant changes on oxidation or reduction of a complex. For the $(\text{mnt})_3$ complexes the determination of the force field is a sizeable problem that requires many independent experimental observations. The difficulties inherent in obtaining sufficiently complete vibrational spectra from transiently stable species makes the complete characterization of the force field and of the redox-based changes thereto impossible at this time. Consequently we have adopted an approach based on the study of bands that arise from well-characterized local modes such as the CN stretch, $\nu(\text{CN})$. This mode is well suited to use in a local-mode approach since it occurs higher in wavenumber than skeletal modes of the ligand ($\nu(\text{C}=\text{C})$, $\nu(\text{CS})$, and the full range of bending modes) and lower in

(19) Hoffmann, R.; Howell, J. M.; Rossi, A. R. *J. Am. Chem. Soc.* **1976**, *98*, 2484.

(20) Kertesz, M.; Hoffmann, R. *J. Am. Chem. Soc.* **1984**, *106*, 3453.

(21) The 24 ligand-based π_v orbitals (each being perpendicular to the mnt plane) of $[\text{M}(\text{mnt})_3]^{2-}$ transform in D_{3h} symmetry as $4a_2' + 4e' + 4a_1'' + 4e''$. These orbitals divide into three sets of eight, $1\pi_v(a_2' + e')$, $2\pi_v(a_1'' + e'')$, $3\pi_v(a_2' + e')$, $4\pi_v(a_1'' + e'')$, $5\pi_v(a_2' + e')$, $6\pi_v(a_1'' + e'')$, $7\pi_v(a_2' + e')$, and $8\pi_v(a_1'' + e'')$, and are filled up to and including $5\pi_v$ for mnt^{2-} . The lowest acceptor orbitals are thus the $6\pi_v$ ones. For a geometry between trigonal prismatic and octahedral (D_3 rather than D_{3h} symmetry), the e' orbital (in D_{3h} symmetry) transforms as e , i.e. in the same way as both the d_{xy} , $d_{x^2-y^2}$ and the d_{xz} , d_{yz} sets.

Schematic Energy Level Diagrams

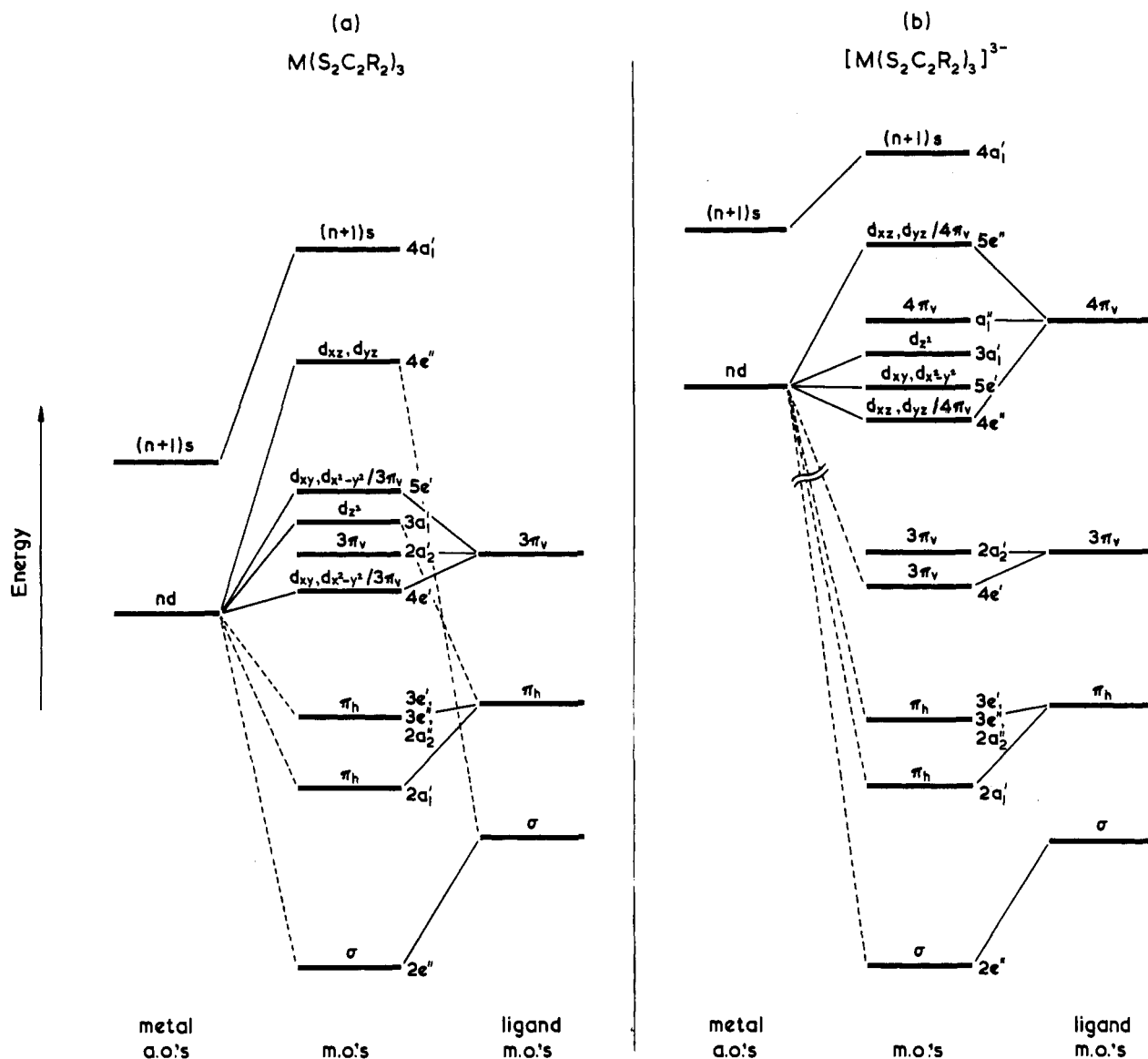


Figure 9. Frontier molecular orbitals for a trigonal-prismatic $M(S_2C_2R_2)_3$ system (after Stiefel et al.¹⁶) and those suggested for $[M(S_2C_2R_2)_3]^{3-}$.

wavenumber than C-H stretching modes.

In the infrared spectrum of the $(mnt)_3$ complexes the $\nu(CN)$ band normally occurs between 2150 and 2220 cm^{-1} and is the only major absorption band in this region (Figures 5-7). The wavenumber, intensity, and shape of the band arising from $\nu(CN)$ are clearly sensitive to the identity of the metal atom and to the charge on the complex.

For the simple hexacyano complexes of first-row transition metals,²² changes in the wavenumber and intensity of $\nu(CN)$ have been shown to depend on changes in the $M-C\equiv N$ bonding. The integrated absorption coefficient (K_6) is a measure of the extent of metal-carbon π bonding. For example, K_6 increases from 18 300 $\text{dm}^3 \text{mol}^{-1} \text{cm}^{-2}$ for $K_3[\text{Co}(\text{CN})_6]$ to 92 000 $\text{dm}^3 \text{mol}^{-1} \text{cm}^{-2}$ for the isoelectronic $K_4[\text{Fe}(\text{CN})_6]$, as the back-donation is much larger for the more highly charged anion. There is also an increase in K_6 on going from $K_3[\text{Cr}(\text{CN})_6]$ ($K_6 = 2100 \text{ dm}^3 \text{mol}^{-1} \text{cm}^{-2}$) to $K_3[\text{Co}(\text{CN})_6]$ ($K_6 = 18 300 \text{ dm}^3 \text{mol}^{-1} \text{cm}^{-2}$) as the number of d electrons on the metal atom available for back-bonding increases. Moreover $\nu(CN)$ decreases with increasing negative charge on the complex, from 2150 cm^{-1} for $[\text{Mn}(\text{CN})_6]^{2-}$ to 1934 cm^{-1} for $[\text{Mn}(\text{CN})_6]^{5-}$. An increase in CN σ bonding will, obviously, strengthen the CN bond and shift $\nu(CN)$ to higher wavenumber. However an increase in π back-bonding from the

metal to the ligand will populate π^* -antibonding orbitals on the cyanide and shift $\nu(CN)$ to lower wavenumber, accompanied by a shift of $\nu(MC)$ to higher wavenumber.

On the basis of these results for simple transition-metal cyanides, variations in the wavenumbers and intensities of the $\nu(CN)$ bands of mnt complexes can be interpreted in terms of changes in the σ and π bonding in these species. We interpret the changes in $\nu(CN)$ in terms of changes in the electron occupancy and the d-orbital contribution to the MO that involves the π_v -acceptor orbital, i.e. the one that includes the π^* orbitals on each cyanide group. This component of the bonding will be more sensitive to the identity of the metal atom and to its formal oxidation state than is the CN σ bonding or other π bonding since the influence of the metal atom on the CN σ bonds must be transmitted through the framework of the mnt ligand; moreover, there is no overlap possible between the CN π orbitals normal to π_v and the metal d orbitals. Hence, the CN infrared chromophore contains information that can be interpreted in terms of the interaction of the ligand π_v orbitals with the metal atom. Changes of the intensity of the $\nu(CN)$ band with the identity of the metal atom will similarly reflect the propensity to back-donation.

The constancy of the wavenumber of the $\nu(CN)$ mode (Figure 10) for the monoanions ($2215.7 \pm 2 \text{ cm}^{-1}$; $M = \text{V, Cr, Mo, W, Re}$) and dianions ($2202.1 \pm 2 \text{ cm}^{-1}$; $M = \text{V, Cr, Mn, Fe, Mo, W, Re}$) is a surprising and important result. It means that the

(22) Jones, L. H. *Inorg. Chem.* 1963, 2, 777.

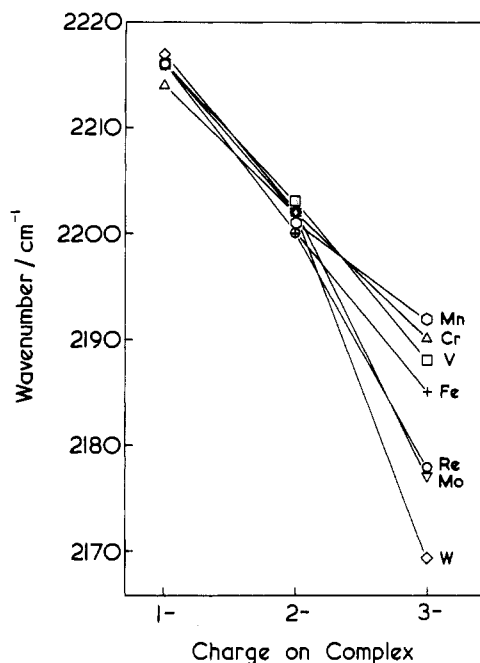


Figure 10. Correlation of the cyanide stretching frequency with charge on the complex.

C—N force constant is insensitive to the d-orbital occupancy (d^0 – d^3 for the monoanions and d^1 – d^5 for the dianions) and to the relative energies of the d orbitals of the first-, second-, and third-row transition metals. Since the influence of the metal atom on the C—N force constant primarily results from changes in the occupancy of the set of π_v orbitals on the mnt ligand, the constancy of the wavenumber of the $\nu(\text{CN})$ mode requires there to be either (a) insignificant overlap between the d orbitals on the metal atom and the π_v orbitals of the mnt ligand or (b) variations in the d-orbital participation in a molecular orbital involving the π_v -acceptor orbital on the mnt ligand (as a result of changes in the d-orbital occupancy and energy) that are exactly balanced by changes in the CN σ -bond strength as a result of changes in the M—S bond strength. The wide range of metals used in this study makes the latter possibility unlikely, an interpretation that is supported by the relatively wide (23 cm^{-1}) variation in $\nu(\text{CN})$ of the trianions. Hence, for the mono- and dianions, the MO scheme that is most appropriate is one that is intermediate between those indicated in Figure 9a,b; i.e., the metal d orbitals lie too far above the ligand π_v HOMO's and too far below their LUMO counterparts for significant interaction to take place in either case.

Since we interpret the infrared spectra to imply that the redox process does not involve the π_v orbitals of the ligand in the case of the mono- and dianions but only the metal d orbitals, we would expect only small changes in the $\nu(\text{CN})$ band on reducing the monoanion. The variation that does occur is explained in terms of the polarizing power of the metal cations, and this will be related to the charge/radius ratio. So while there is no evidence for charge delocalization to the metal for the mono- and dianions via a π -type interaction, there is evidence for charge redistribution within the π_v orbitals of the ligand as a result of changes in the polarizing power of the metal ion.

For the trianions the wavenumber of the $\nu(\text{CN})$ mode is lower than for the dianions and it is, by contrast to the situation for the mono- and dianions, sensitive to the identity of the metal atom, spanning 23 cm^{-1} for the range of metals studied. Significantly, $\nu(\text{CN})$ for the first-row metals is greater than those for the second-

or third-row metals. This sensitivity of the wavenumber of $\nu(\text{CN})$ to the identity of the metal atom is matched by variations in the relative intensities and half-widths of the $\nu(\text{CN})$ bands. These observations are in keeping with an increased metal contribution to the molecular orbital involving the lowest π_v -acceptor orbital of the mnt ligand, with increased negative charge on the anion. This increased metal participation arises because (vide supra), with the addition of electrons to the metal center, the d orbitals increase their energies until, for the trianions, they are close to that of the lowest unoccupied set of π_v orbitals of mnt (arbitrarily referred to as $4\pi_v$ in Figure 9b). Thus, we consider that it is the formal oxidation state of the metal ion (and hence the overall charge on the anion) rather than the number of d electrons that determines the extent of d-orbital participation in the π_v -acceptor orbital of the mnt.

In addition to the CN stretching mode, other vibrational modes of the complex give rise to bands whose wavenumber ought to be interpretable in terms of particular force constant changes. The M—S, C=C, and C—S stretching modes, for example, should provide a source of complementary information for the identification of changes in the complex as a result of oxidation or reduction. In this study we have examined the bands arising from these modes. For the C=C and C—S modes the breakdown of the local-mode approximation, through coupling, and the presence of strong absorptions of solvent and/or supporting electrolyte in the same spectral region combine to limit the useful information obtainable in this region. However, for the M—S stretching modes these problems are less severe and, from the spectra obtained in the M—S stretching region (Figure 8), it is evident that $\nu(\text{MS})$ moves, as expected,²³ to lower wavenumber on one-electron reduction (by ca. 20 cm^{-1}). For $[\text{Re}(\text{mnt})_3]^-$ the shift of $\nu(\text{MS})$ is approximately equal for the first and second reductions. In order to establish further the variation of $\nu(\text{MS})$ with the formal oxidation state of the metal atom, we need to extend this aspect of the work to a wider range of metals.

Conclusion

The purpose of this work was to establish the nature of the frontier orbitals of certain $(\text{mnt})_3$ complexes and thus to clarify the role of mnt in modifying the redox chemistry of the transition-metal ion to which it is complexed. In practice, the infrared rather than the electronic spectroelectrochemical results proved to be the more informative, the trends in $\nu(\text{CN})$ being explained—in part—in terms of the increasing extent of π back-donation from the metal d_π orbitals into the π_v -antibonding orbital involving the cyanide groups with increasing negative charge on the anion. Thus it is the charge on the anion that is the key factor which determines $\nu(\text{CN})$, since this determines the metal orbital energies and thus the energy match between the d_π and the π_v -acceptor orbitals.

We conclude that, for $[\text{M}(\text{mnt})_3]^{z-}$ species in which $z = 0$, the stabilization probably occurs via both M—S σ bonding and $\text{mnt} \rightarrow \text{M}(d_\pi)$ π bonding, and for those in which $z = 1$ or 2 , it occurs overwhelmingly by M—S σ bonding, while for $z = 3$, the metal center is sufficiently electron rich for $\text{M}(d_\pi) \rightarrow \text{mnt}(\pi^*)$ back-bonding to become significant.

Acknowledgment. We thank the SERC for the award of grants to R.C.S.M. and J.R.W.

Registry No. $[\text{AsPh}_4]_2[\text{V}(\text{mnt})_3]$, 12114-37-3; $[\text{PPh}_4]_3[\text{Cr}(\text{mnt})_3]$, 20589-25-7; $[\text{PPh}_4]_2[\text{Mn}(\text{mnt})_3]$, 20584-90-1; $[\text{PPh}_4]_2[\text{Fe}(\text{mnt})_3]$, 17786-38-8; $[\text{NBu}_4]_2[\text{Mo}(\text{mnt})_3]$, 19582-22-0; $[\text{PPh}_4]_2[\text{W}(\text{mnt})_3]$, 20523-82-4; $[\text{PPh}_4]_2[\text{Re}(\text{mnt})_3]$, 112571-39-8.

(23) Clark, R. J. H. *Spectrochim. Acta* **1965**, *21*, 955.